Title
Developing MODIS-based cloud climatologies to aid species distribution modeling and conservation activities

Permalink
https://escholarship.org/uc/item/0247q946

Journal

Authors
Douglas, Michael William
Beida, Rahama
Mejia, John F.
et al.

Publication Date

DOI

Supplemental Material
https://escholarship.org/uc/item/0247q946#supplemental

Copyright Information

Developing MODIS-based cloud climatologies to aid species distribution modeling and conservation activities

Michael W. Douglas[1,*], Rahama Beida[1], John F. Mejia[2], and Marcia Fuentes[3]

[1]CIMMS/University of Oklahoma, Norman, Oklahoma, USA; [2]Desert Research Institute, Reno, Nevada, USA; [3]IFSC Meteorologia, Florianopolis SC, Brazil; *douglasnoaa@gmail.com

Abstract. WorldClim (Hijmans et al. 2005) has been the de-facto source of basic climatological analyses for most species distribution modeling research and conservation science applications because of its global coverage and fine (<1 km) spatial resolution. However, it has been recognized since its development that there are limitations in data-poor regions, especially with regard to the precipitation analyses. Here we describe procedures to develop a satellite-based daytime cloudiness climatology that better reflects the variations in vegetation cover in many regions of the globe than do the WorldClim precipitation products. Moderate Resolution Imaging Spectroradiometer (MODIS) imagery from the National Aeronautics and Space Administration (NASA) Terra and Aqua sun-synchronous satellites have recently been used to develop multi-year climatologies of cloudiness. Several procedures exist for developing such climatologies. We first discuss a simple procedure that uses brightness thresholds to identify clouds. We compare these results with those from a more complex procedure: the MODIS Cloud Mask product, recently averaged into climatological products by Wilson and Jetz (2016). We discuss advantages and limitations of both approaches. We also speculate on further work that will be needed to improve the usefulness of these MODIS-based climatologies of cloudiness. Despite limitations of current MODIS-based climatology products, they have the potential to greatly improve our understanding of the distribution of biota across the globe. We show examples from oceanic islands and arid coastlines in the subtropics and tropics where the MODIS products should be of special value in predicting the observed vegetation cover. Some important applications of reliable climatologies based on MODIS imagery products will include 1) helping to restore long-degraded cloud-impacted environments; 2) improving estimations of the spatial distribution of cloud-impacted species; and 3) helping to identify areas for rapid biological assessments. The last application can even benefit from qualitative perusal of the current MODIS climatologies.

Keywords. Climate, remote sensing , MODIS, species distribution modelling, conservation

Introduction

Motivation

Determining the true range of any species is an essential component of conservation biology. Unless the range of a species is accurately known, the most cost-effective solutions to its long-term protection cannot be determined. Integrating over all known species distributions provides a map of biodiversity, which can likewise be used to help strategize conservation of the most species for the least cost.

Key to the estimation of any species' distribution is relating its known (observed) occurrence to environmental conditions that are thought to control its presence (or absence). Predictions of where it is likely to be found can then be made –

greatly reducing the task of field sampling. While some environmental variables, such as elevation and slope aspect, have become accurately known with recent satellite information, other environmental conditions remain poorly known. In particular, climatological observations remain very unevenly distributed across the globe, with biota-rich tropical regions often being the most poorly described by routine climatic observations.

The source of climatological data most widely used by the niche modeling and conservation biology community is WorldClim1.4 (Hijmans et al. 2005). This was produced by interpolating monthly mean climate data from nearly 50,000 stations to a 2 km spatial grid with a procedure that incorporated high-resolution topographic

information. The widespread use of WorldClim1.4 is evident by its more than 8800 citations to date[1]. Despite this near-ubiquitous use among biogeographers, there is awareness within the research community that some WorldClim1.4 products, such as those related to precipitation, are not sufficiently accurate for many applications.

In this paper, we discuss climatologies of cloudiness that can be developed from twice-daily high-resolution observations from two sun-synchronous satellites carrying the Moderate Resolution Imaging Spectroradiometer (MODIS) instrument[2]. The technique we have used to produce cloud climatologies is somewhat different from a procedure recently presented by Wilson and Jetz 2016 (hereafter WJ2016). Though both procedures yield similar results in many areas, there are important differences. We discuss both techniques, focusing on their advantages and limitations for obtaining cloudiness estimates and also speculate on how the procedures can be improved to make the resulting products more useful to the conservation and biogeographical research communities.

The importance of clouds to the biological environment

It is intuitively apparent that cloud cover affects the Earth's surface daytime temperature. Cloudy days are cooler than sunny days, other factors being equal. This is most obvious in subtropical and tropical locations where high values of daytime solar radiation exist throughout the year and where temperature variations between one sunny day and the next are usually small. Since cloud cover reduces incoming solar radiation and thus the surface temperature, and since the maximum daytime temperature affects the potential evapotranspiration from a land surface, variations in cloud cover should impact the underlying vegetation. Thus, describing the mean daytime cloud cover should be of value in helping to explain the Earth's vegetative cover.

Since daytime MODIS imagery is available only at two times near local noon, it is natural to ask why such a limited data set may be valuable. One can argue that daytime cloudiness is more important for most biological processes than cloudiness at night. Thick clouds can strongly reduce incoming solar radiation; this effect is a function of the solar zenith angle, with maximum modulation at local noon and very little impact near sunrise and sunset. Thus the two MODIS overpass times, about 1.5 hours on either side of local noon, provide cloud information when incident solar radiation is near its maximum. Surface (ground) temperature, near-surface air temperature and surface evaporation are all strongly affected by this mid-day cloud modulation of incoming solar radiation. In contrast, clouds at night only affect the outgoing longwave (infrared) radiation, which affects the minimum temperature that may be reached. While this can be important for some biota, the effect on evaporation and transpiration will be much less than with daytime cloud cover. Lower night-time temperatures are associated with higher relative humidities. As surface evaporation is primarily a function of air temperature, relative humidity and surface wind speed (which is generally much less at night over tropical land areas), it follows that the surface evaporation is generally much less at night.

In summary, cloudiness around local noon has a disproportionate impact on the potential aridity[3] of a tropical land surface because of its strong role in modulating evapotranspiration – compared with cloudiness at night or during the early morning or late afternoon hours. Therefore, a climatology of MODIS-based mid-day cloudiness should be useful as an aid in explaining the distribution of vegetation patterns and their associated biota.

The next section (Section 2) discusses MODIS data and some of their characteristics. The procedures used to develop cloud frequency climatologies are also covered, including limitations

---

1 Google Scholar showed 8823 citations as of September 14, 2016
2 http://modis.gsfc.nasa.gov, last accessed September 14, 2016
3 potential aridity can be defined as a ratio of precipitation to potential evapotranspiration with arid regions having values less than one. Many variants of this definition exist.

of the techniques. In Section 3 we compare our threshold-based climatological products with those of the very recent extensive effort by WJ2016. In Section 4 we describe some products not covered in WJ2016. Finally, in Section 5 we recap our perceptions of the key findings, and provide some suggestions for necessary future work to make MODIS-based cloud climatologies more valuable.

Data sources and processing

Overview of the data and cloud climatology development

We have used MODIS visible imagery from two sun-synchronous NASA satellites, Terra (10:30 local time (LT) equator overpass) and Aqua (13:30 LT equator overpass). These satellites also have night-time overpasses but we have not attempted to determine cloudiness at these times because 1) visible imagery is not available (which provides the highest spatial resolution) and 2) there are complications in uniquely identifying low clouds at night from available infrared imagery over land surfaces. The temporal coverage of the daytime imagery from the two satellites, taken together, provides a reasonably good estimation of mid-day cloudiness.

The use of MODIS imagery allows for the development of climatologies of cloudiness at higher spatial resolution than commonly available. For example, the International Satellite Cloud Climatology Project[4] (ISCCP) spatial resolution is now 1 degree lat/long, though other climatologies are finer (e.g. 36 km in Karlsson (2003) and 30 km in Stubenrauch et al. (2010), see Stubenrauch et al. (2013) for a summary of recent cloud climatology products). These coarser resolutions are acceptable for global and large-scale climate studies but are not as useful for relating cloudiness to small-scale topographic features, especially in the tropics. MODIS visible imagery, with a resolution of up to 250 m, affords *in principle* many times higher spatial resolution.

MODIS data can be obtained from various NASA data centers and many atmospheric products have been generated with the aid of different algorithms. One such product is the MODIS cloud mask (Platnick et al. 2003), which provides users with an estimate of the likelihood of clouds (many users need to know whether the view of the Earth's surface is obstructed by clouds, smoke or dust). We have not used the MODIS cloud mask product because 1) we initially judged it to have serious artifacts associated with land surface features (see Wilson et al. 2014 for discussion of these problems) and 2) the cloud mask product pixel resolution was 1 km, compared with 250 m in the full resolution imagery. Instead, we used sectors already defined for various parts of the world and available online from NASA[5]. These images, already accurately navigated and with sufficiently small pixel dimensions for processing on a personal computer, were downloaded at full (250 m) resolution as input data for development of MODIS cloud frequency climatologies.

The MODIS 'true color' images, comprising MODIS spectral channels 1, 4 and 3 (see specifications[6]) were downloaded as Joint Photographic Experts Group (JPEG) imagery from the NASA Earth data portal[7]. This online data set has different start dates for different geographical sectors – depending on the user community. We stress that our climatological products discussed here, though multi-year, do not use the full MODIS observation record, nor are they global in coverage. They were developed for specific regions using some of the available subsets. However, the procedures we have used, and the importance of the products derived from them, can be applied equally to a more complete processing effort.

Missing data from portions of the images often occurred because of non-overlapping satellite swaths at lower latitudes and these areas were detected (by their brightness of 255 in all three color channels) and ignored in the cloud

---

frequency calculations. The images were then processed to distinguish the cloudy from non-cloudy pixels in each image. This was done by converting the original true color images into an 8-bit grayscale image with the luminance formula (Kanan and Cottrell 2012):

8 bit grayscale value = (0.299 * Red + 0.587 * Green + 0.114 * Blue)

and then applying a brightness threshold of 215 (0=black, 255=white) and above to select the 'cloudy' pixels. These 'cloud mask' images were then averaged over individual months and these monthly means were used to generate seasonal means of cloud frequency. As a first pass, we produced means of the boreal warm season (Nov–Apr) and cool season (May–Oct) from which we produced annual means. Individual yearly means were then averaged to produce multi-year means of the various cloud frequency products.

Despite the simplicity of the above approach, there are subtleties in the procedures to detect clouds and to time-average the cloudiness fields. These are described in the next subsections.

Choosing the proper threshold to detect clouds

The initial threshold chosen to identify thick (highly reflective) clouds was based on tests that showed that a value of 215 would be high enough to not detect smoke that was prevalent over parts of South America during the dry (burning) season. Unfortunately, this value was later noted to underestimate the amount of low stratus clouds, especially in the areas offshore from the Californian, Peruvian, and Namibian coasts. Using a value near 170 effectively captured most of the thicker (brighter) stratus clouds, but the brighter land surfaces inland over these dry regions are then often counted as cloudy pixels. Figure 1 illustrates this fundamental challenge to cloud detection efforts using any threshold procedure based on visible imagery. In principle, the cloud-detection threshold can be varied with the intended objective and the expected contamination from the underlying surface.

Where glaciers, salt flats, and bright sandy areas are present it is not possible to accurately estimate the cloud frequencies because their background brightness will exceed the threshold
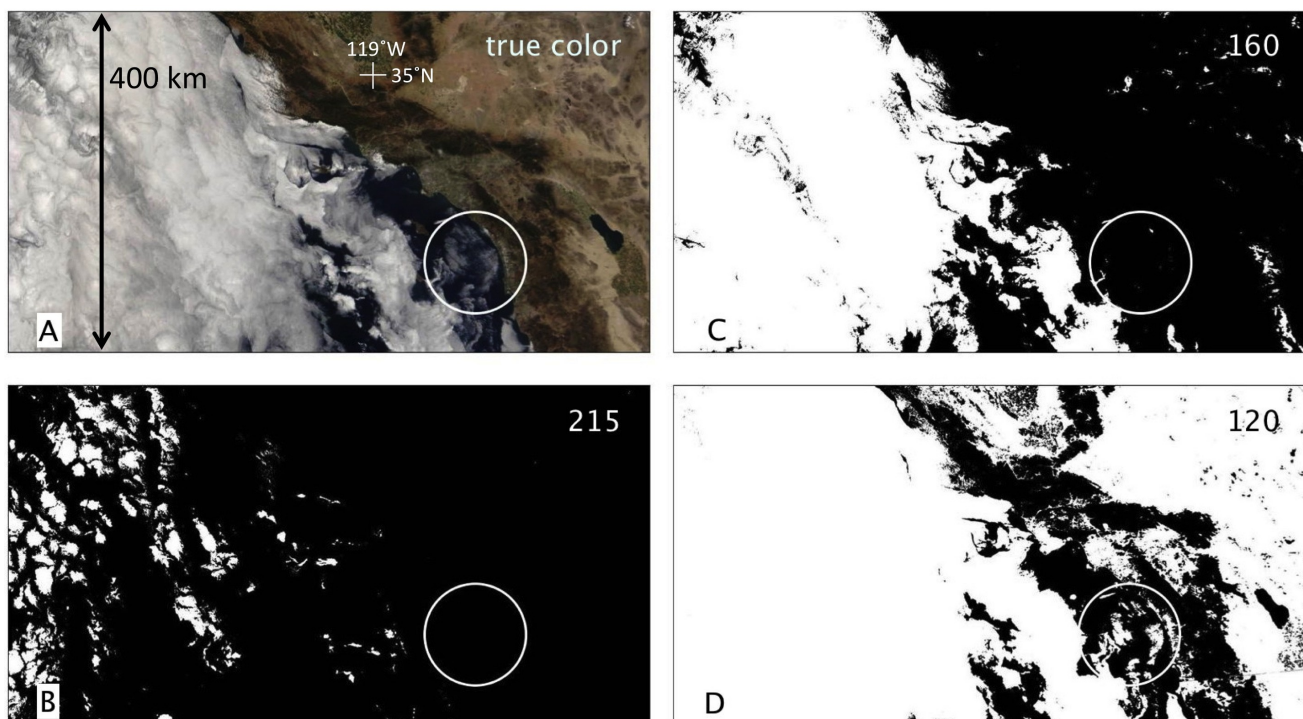
Figure 1. MODIS True-color image and successive cloud masks obtained by applying different cloud detection thresholds. a) Original MODIS Terra true-color imagery for the Southern California region showing stratus clouds of varying reflectivity (thickness); b) cloudy pixels detected by using a grayscale threshold of 215; c) clouds detected using a 160 threshold; d) clouds detected using a 120 threshold. Note the increasing detection of cloud-free land areas in c) and d). The circle encloses thin stratus clouds that are not detected except at the lowest (120) threshold.

values for clouds. However, ice fields are of very small spatial extent in the tropics and subtropics, and, like salt flats and extensive sand dune fields, are regions of minimal biodiversity, so perhaps a greater uncertainty in estimating cloudiness in these regions is acceptable for biogeographical applications.

The most serious limitation to any simple thresholding procedure is found in the mid-latitudes, where snow may cover the surface for extended periods in the cool season. A fresh snow surface is highly reflective and may exceed a chosen cloud detection threshold. There is no simple procedure for separating snow from low clouds with a visible imagery-based algorithm. Thus, our procedure for developing cloud frequency climatologies has a geographical and temporal restriction – it cannot be applied reliably to regions where snow cover is present for appreciable periods. Despite this, there are some regions at higher latitudes where snow is rare, such as the oceanic fringes of Western Europe and the coastal regions of South America and Australia. If the climatology of snow is known accurately, then the procedure can be applied to snow-free or snow-rare regions even during the cool season.

Why use a 'simple' thresholding technique?

While an initial version of this paper was undergoing review, a longer (15-year) average of the MODIS-derived cloudiness appeared (Wilson and Jetz 2016, or WJ2016), along with many quantities derived from the monthly mean cloudiness. Because their climatological products use the full record from the MODIS instruments, have global coverage, and are presented in a user-friendly format for immediate application by the research community, we initially thought their work obviated the need for our manuscript. In fact, the convenient format and availability of their products have allowed us to make a relatively rapid comparison of our products with their results. Here, and especially in Section 3, we describe aspects of this comparison.

Why use a simple cloud detection algorithm when a more complex cloud detection procedure exists (MOD09 cloud mask products; see Vermote et al. 2011), whose results have already been averaged to produce the relatively complete MODIS cloud climatology of WJ2016? To anticipate our findings presented below, the WJ2016 products suffer from important deficiencies. Based on our comparisons, the most important reasons to consider a simple threshold-based cloud climatology are 1) to minimize surface albedo-related artifacts present in the MOD09 products, 2) to discriminate thick clouds from thin clouds and 3) to obtain greater spatial resolution (250 m) compared with the MOD09 product (1km). Though not specific to our threshold technique, maintaining the Terra and Aqua results separately (WJ2016 merged the two) is useful since their difference contains valuable information on the diurnal cycle of cloudiness. It may be important to know whether morning and afternoon cloudiness differ, and by how much.

While details of the MOD09 algorithm have been summarized in WJ2016, it is important to reiterate two aspects of those MODIS cloud mask procedures. Firstly, the primary purpose of developing the MOD09 (or similar) cloud mask product is not to characterize clouds, but rather to assure users of surface reflectance data that scenes are unobstructed by clouds (or thick dust[8] or smoke; Platnick et al. 2003). Secondly, as Wilson et al. (2014) and WJ2016 note, the available MODIS cloud mask products do not discriminate between types of clouds or their thickness. *Even a highly reliable cloud detection algorithm does not necessarily yield a product useful for applications in biogeography or ecology.* Why? Because not all clouds have the same impact on the underlying surface. Consider the following example. Though thin cirrus may be readily detected by the MOD09 cloud mask algorithm, these clouds, perhaps 10 km above the surface, may not block much daytime solar radiation. The surface humidity beneath the cirrus may be quite low despite the presence of near-saturated conditions at the level of the cirrus. Low stratus clouds, on the other hand, often are thick enough to block most sunlight (reducing daytime surface

---

8 That the MOD09 product detects thick dust can be seen by examining the dust plume signature extending westward from the Bodélé depression (~17˚ N, 18˚ E) in Chad.

temperatures), may provide fog-drip on vegetated slopes (a liquid water source), and also immerse the vegetation in a near-saturated atmospheric environment (reducing transpiration). Thus, although both thin cirrus and the thick stratus may be detected with confidence as a 'cloudy pixel', they can have vastly different impacts on the underlying vegetation. The results of WJ2016 cannot distinguish between such cloudy pixels. On the other hand, thin (low reflectivity) clouds can be selectively eliminated from detection by using a high reflectivity threshold (Figure 1). This can eliminate thin low stratus, thin high cirrus or thin mid-level clouds – the result cannot be predicted. The only assurance is that pixels representing thick, highly reflective clouds will be retained. A mean cloudiness field obtained in this way is likely to have a closer relationship with the surface vegetation. Actually showing this – that areas with maximum frequency of highly reflective pixels are more closely related to the underlying vegetation cover and possibly to precipitation, can only be meaningfully done on a local scale (not with global statistics), because the relationship between mean cloudiness

and precipitation varies strongly across the globe.

In the next subsection we discuss some of the differences between products derived from our thresholding procedure and that carried out by WJ2016 using the MOD09 cloud mask products. To anticipate our conclusions – both procedures yields products that should not be used without a clear understanding of their limitations. This reiterates the conclusions of Wilson et al. (2014) regarding an earlier cloud mask product.

Comparison of the mean cloud mask and threshold products

Time averaging of the daily MOD09 or threshold-based products is an effective procedure to identify subtle problems that might not be apparent in the daily products. Since our thresholding products have been developed with an incomplete record of the MODIS period of observations, the stability of our mean cloudiness features might be questioned. The data show that for many locations with strong topographic forcing of cloudiness, only short periods are needed to represent
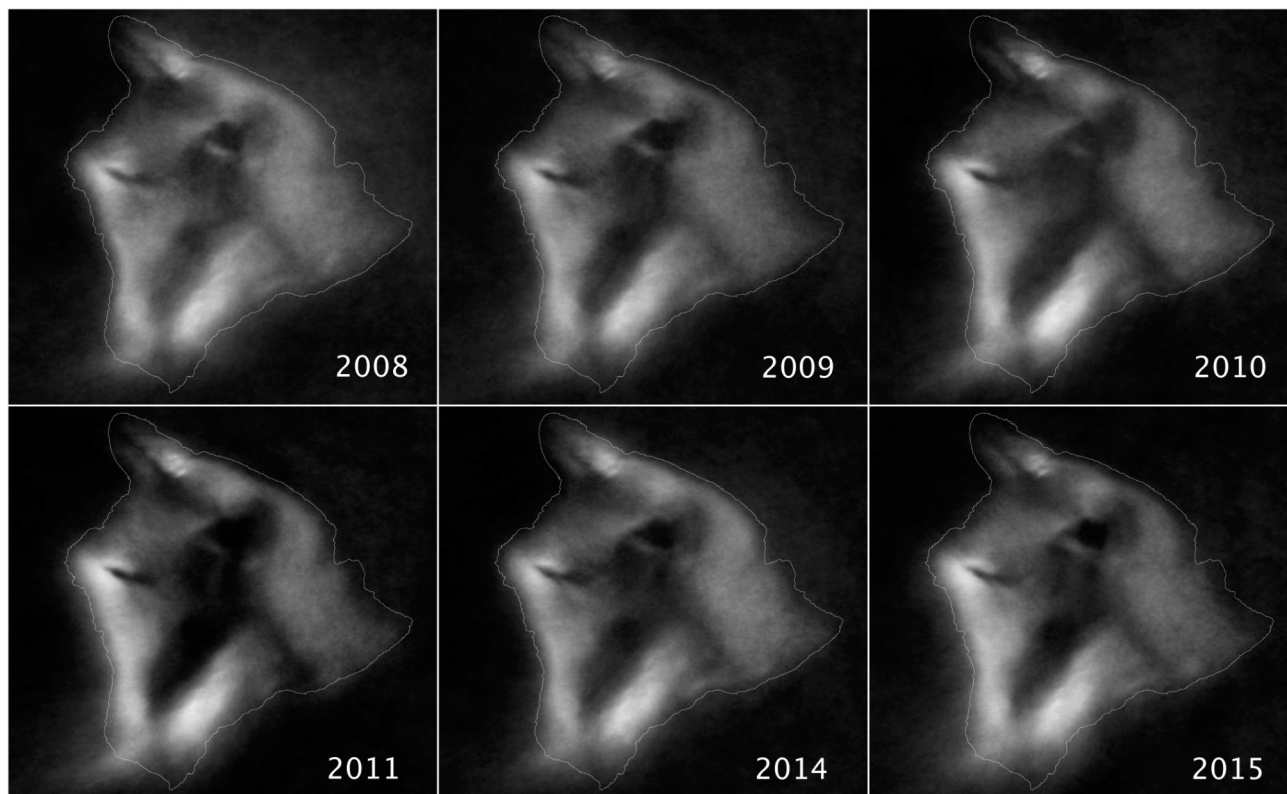
Figure 2. May through October mean cloudiness for six different years for the island of Hawaii from MODIS 215-threshold product. Years 2012–2013, were similar but had some missing observations in our data base and are not shown. *All of the main features in the cloud field are evident in each year*.
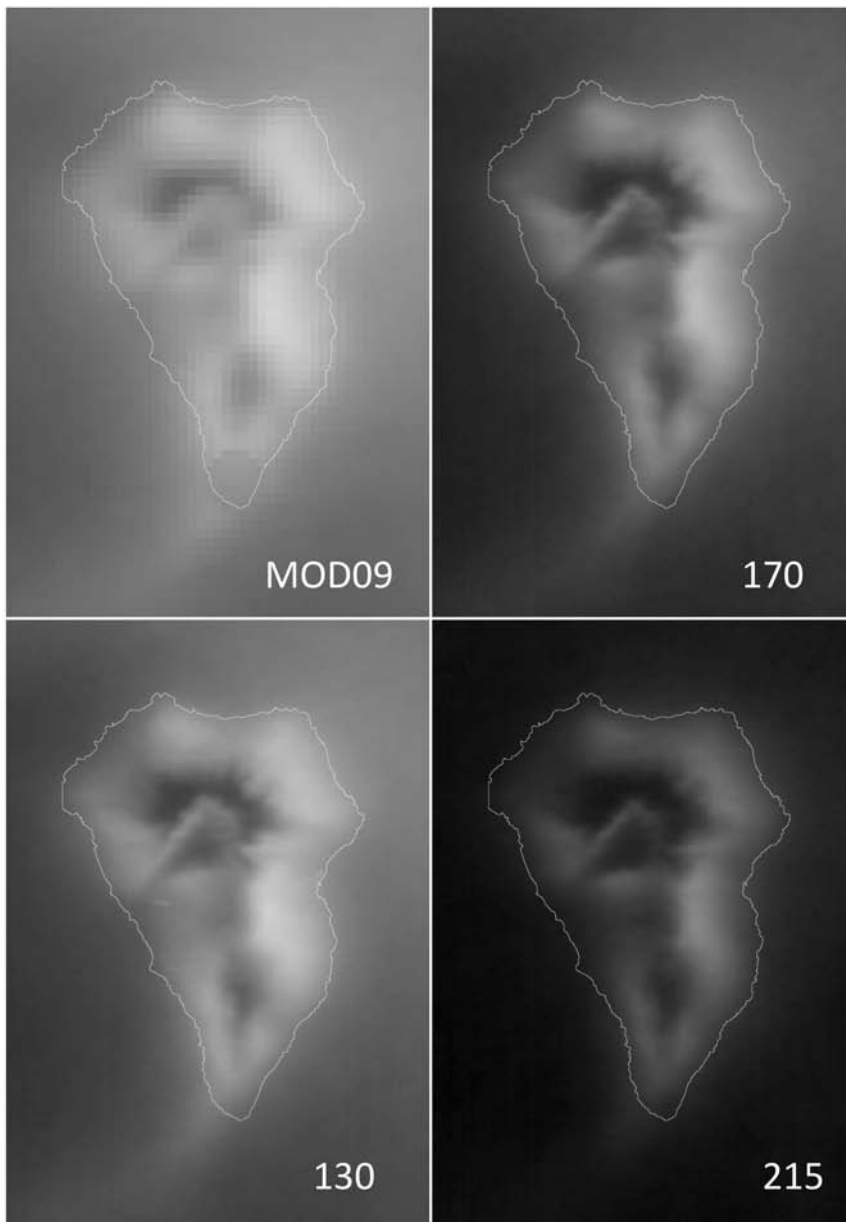
Figure 3. MODIS-based annual mean cloud climatologies for the island of La Palma in the Canary Islands. The MOD09 is from WJ2016, grayscale is from 0 to 100%. The other panels are for different threshold values for a 6-year period of observations. Grayscale is 0 to 100% for each of these; the 215 threshold detects the least cloudiness. Minor surface artifacts are present in the 130 threshold. Though the threshold procedure detects differing amounts of cloudiness with different thresholds, the same patterns are evident in each average. Also note the finer-scale features evident in the threshold averages. A high-resolution version of this figure is available in the online Supporting Material.

the important cloudiness gradients (Figure 2). In arid, cloud-sparse regions, longer averaging periods would clearly be needed.

As a first impression, over many continental areas, the threshold-based mean cloudiness patterns are often very similar to those of WJ2016, though the percentage of cloudy pixels is much higher in the WJ2016 results than with our 215 threshold products. This is expected, since the objective of the MOD09 algorithm is to detect even thin clouds, as well as appreciable dust and smoke. Our 215-thresholding procedure intentionally does not detect low-reflectivity clouds.

Comparisons of cloud frequency determined by three thresholds (215, 170, 130) with those from WJ2016 for the island of La Palma in the Canary

Islands are shown in Figure 3. The actual cloud frequency values are much higher in the MOD09 product than with the 215 threshold, but the patterns are similar. A 170 threshold yields values closer to those of the MOD09, but still not as high. Because the mean cloudiness from WJ2016 are much higher, the cloudiness gradients tend to be less those obtained using the threshold technique.

Ice-, salt flat-, and sand dune-related artifacts are evident in the threshold analyses. For this reason the technique is not suitable for most high-latitude or wintertime mid-latitude applications. Despite the complexity of the MODIS cloud mask algorithm relative to the thresholding procedure, the WJ2016 products also show many of the same artifacts. Surface albedo-related artifacts apparent
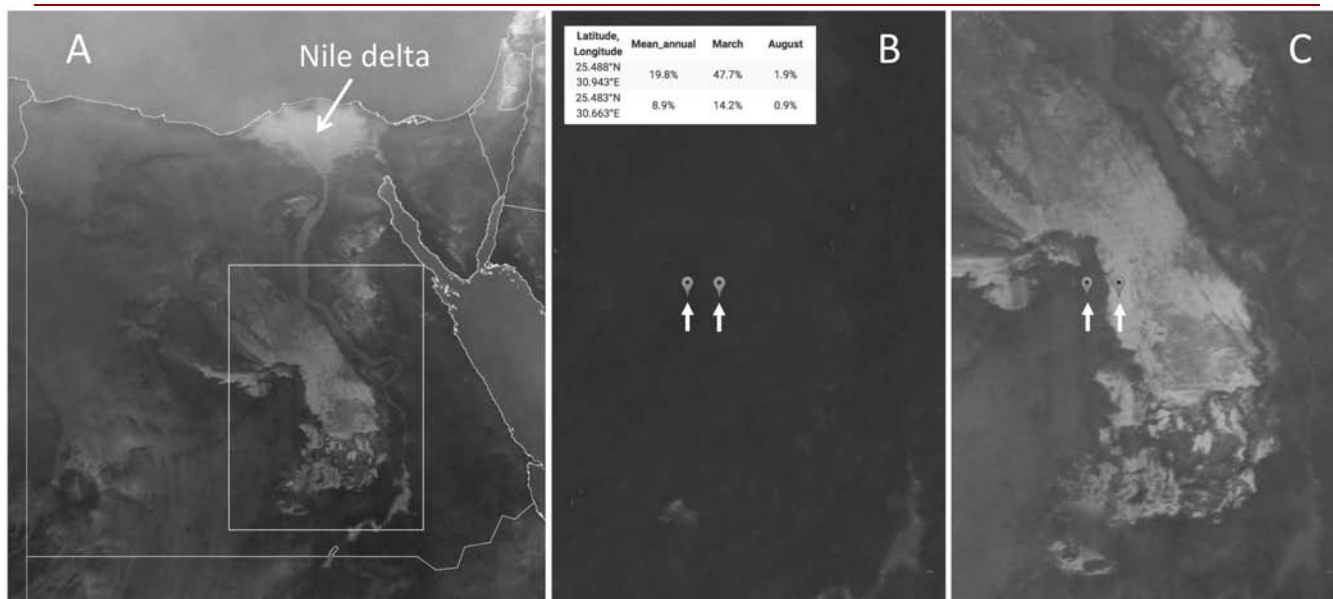
Figure 4. Example of surface albedo-associated artifacts over the Sahara Desert. a) MOD09 WJ2016 annual mean cloudiness for Egypt. Grayscale is between 0 to 50% cloudiness. b) A larger view of the rectangular area shown in a) with August mean cloudiness shown (same grayscale as in a). c) Same as b), but for March. Large seasonal change in cloudy pixels is evident, as are the patterns associated with varying surface albedo. The two arrows indicate locations separated by 28 km. The values of cloudiness at these locations are shown in b) and for August they differ in mean cloudiness by 1%; for March they differ by 33% . The Nile delta cloudiness maximum does not appear in a 215-threshold climatology.

in the mean annual cloudiness fields shown in WJ2016 include Iceland's permanent ice fields, islands and shallow water of the Great Barrier Reef off northeastern Australia, and a great many seasonal or permanent snowfields on higher mountains in parts of Asia, Europe and the Americas. Surface artifacts dominate much of the Sahara Desert (Figure 4) and also the Arabian Peninsula. At a finer spatial scale, cities surrounded by forested regions or farmlands in eastern China and in the southeastern US stand out prominently in the July mean cloudiness fields of WJ2016 (not shown). A 215-threshold product does not show these, indicating that (at least) highly reflective clouds do not preferentially form over cities in these regions.

Seasonal snowfield contamination of the MOD09 and threshold products is not restricted to high latitudes. The mean annual cloud frequencies are particularly misleading in some areas of key biodiversity where the higher spatial resolution potential of MODIS imagery is needed. Figure 5 shows the mean cloudiness for the region of the southern Caspian Sea for a winter and summer month, together with the annual mean cloudiness. Maximum MOD09 frequencies (and also threshold-based cloudiness products) strongly reflect snow cover

over the highest terrain in winter, while summer clouds are generally low and confined to north of the high terrain. Together, the annual mean cloudiness appears continuous and extending to the highest peaks. This contamination of the mean annual cloudiness with wintertime high altitude snow-covered terrain artifacts is also evident other botanically-rich (Barthlott et al. 2005) regions of humid temperate forest bordering the eastern Black Sea and in areas of subtropical forest along the eastern Andean slopes in northwestern Argentina.

The seasonally dry forests on the peripheries of the African and South American evergreen tropical forests are perhaps the largest biota-rich regions in WJ2016 that are adversely affected by surface albedo artifacts. Figure 6 shows a comparison of mean annual cloudiness over the south-central Amazon Basin from WJ2016 and from applying a 215 threshold to seven years of twice-daily MODIS imagery. A remarkable similarity between the deforested regions and the WJ2016 cloudiness is evident, whereas the 215-threshold product shows little such relationship. Rather, the regions of enhanced daytime cloud frequency in the 215-threshold product are associated with hills and low mountains across the domain – as is observed over
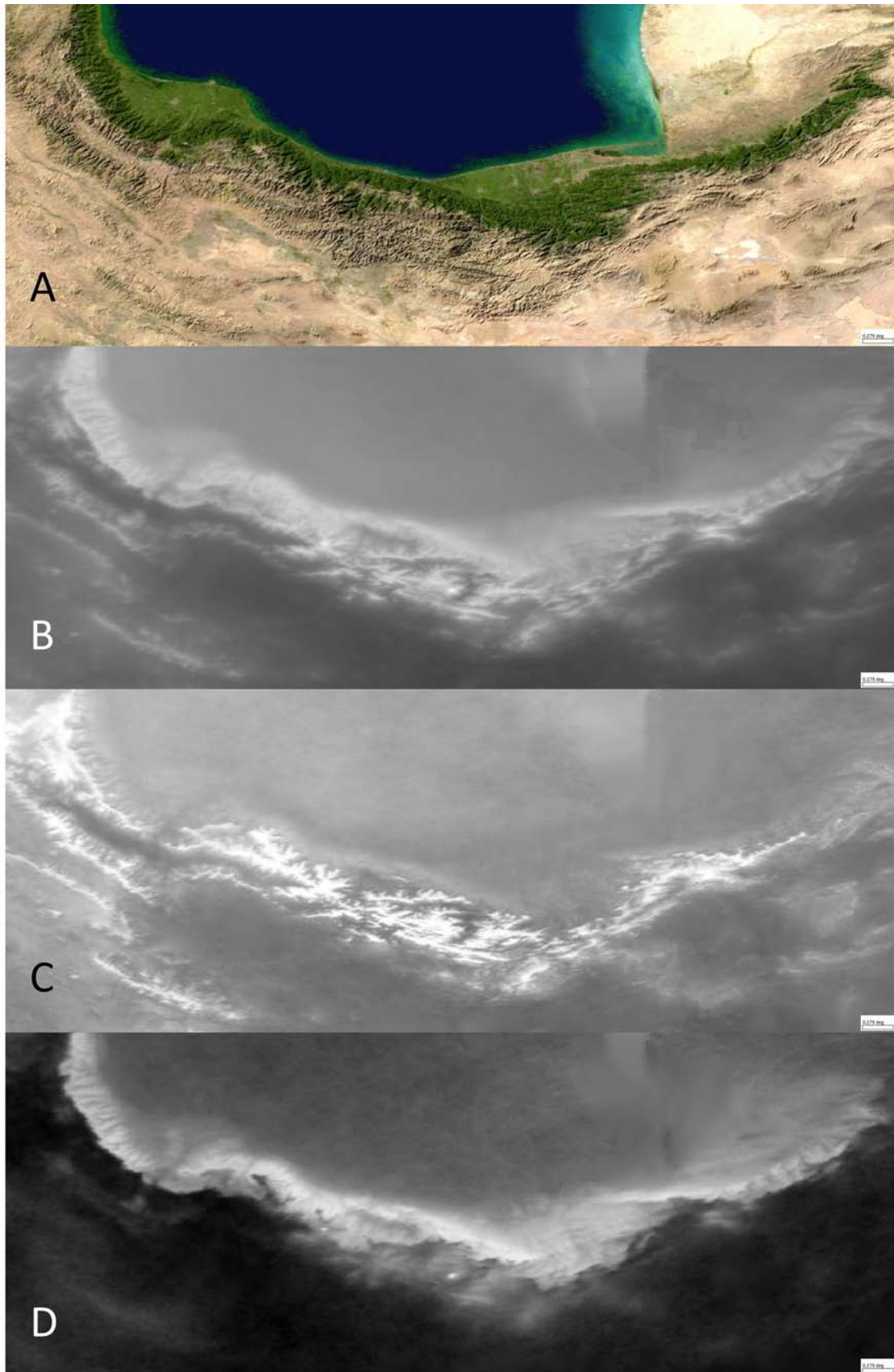
Figure 5. Annual mean cloudiness from MOD09 WJ2016 product at south end of the Caspian Sea. a) True color map showing vegetation cover, b) mean annual cloudiness, c) February mean cloudiness detecting snow cover over higher terrain of the Elburz Mountains, d) July mean cloudiness showing frequent cloudiness on lower slopes of mountains. The annual mean cloudiness can be seen to be a summation of winter cloudiness (mostly detecting persistent snow cover) and summer low cloudiness north of the Elburz Mountains. Distance across images is ~710km.

most landmasses in the humid tropics.

The final important difference between our threshold procedure and that of WJ2016 is that we use the full (250 m) resolution MODIS imagery. Despite the very substantial computational effort to process the 1 km data for WJ2016, a full-resolution data effort might be 16 times larger. For many applications the additional detail evident in the 250 m MODIS data is probably not essential, but Figure 7 (and Figure 3) shows where the additional detail of full resolution is apparent.

Also more apparent on small spatial scales is the smoothing that appears in many parts of the WJ2016 analyses (center image in Figure 7). These are presumably associated with an effort, stated in WJ2016, to reduce surface albedo-related artifacts. These corrections are most common in high albedo areas, such as along coastlines and over salt flats, but are surprisingly widespread.

Products derivable from MODIS imagery

Because WJ2016 have already presented a thorough description of many of the possible products derivable from monthly mean cloudiness data, we focus here on one product that they did not examine. WJ2016 averaged together the monthly mean cloudiness obtained from the Terra and Aqua satellites to produce their monthly (and annual) mean cloudiness products. Thus, they could not describe diurnal changes in the mean cloudiness fields. Here we focus on the value of such products.

### Mean cloudiness from the Terra and Aqua imagery

The simplest MODIS-based cloud frequency product is one using either the Terra (10:30 LT) or Aqua (13:30 LT) imagery. Over land areas there can be clear differences between these mean cloudiness fields that reflect the typical evolution of a daytime
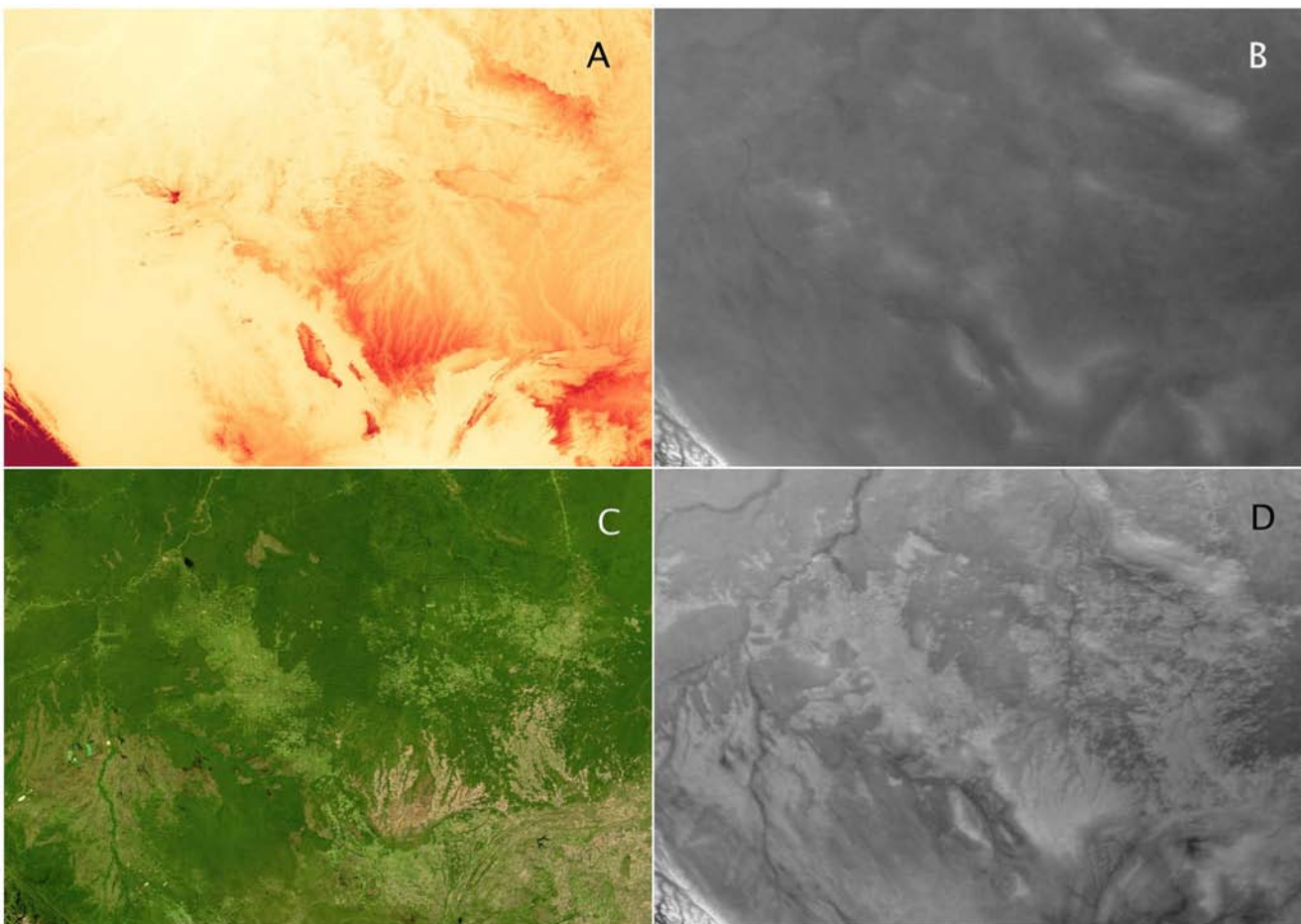
Figure 6. Region of SW Amazonia (images centered near 11.5˚ S 60˚ W, scene is ~1500 km across). A) elevation (0–1200 m scale, red is higher), b) cloudiness from 215-threshold product, c) approximate surface albedo/true color view and d) MOD09-based annual mean cloudiness from WJ2016. Note 1) the close agreement between relief features in a) with areas of maximum cloudiness in b) and 2) close agreement of albedo features in c) with MOD09 cloudiness in d). A high-resolution version of this figure is available in the online Supporting Material.
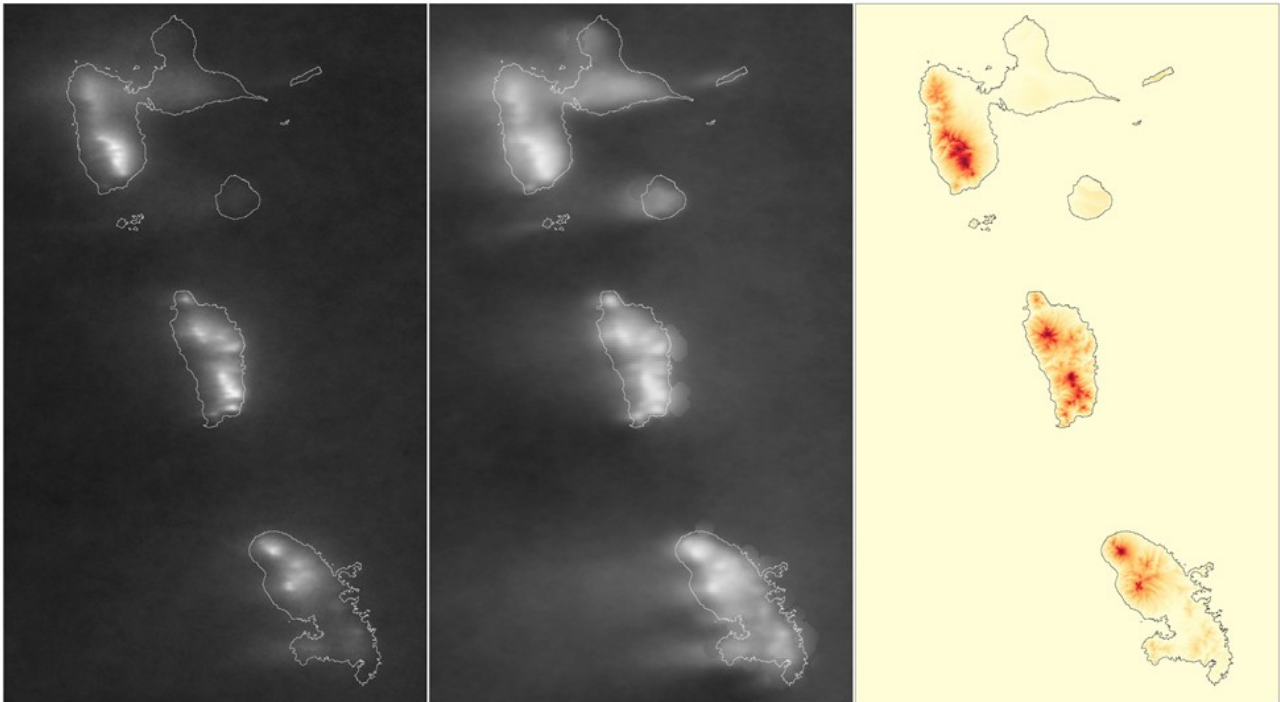
Figure 7. Mean annual cloudiness for some of the Lesser Antilles, from Guadaloupe (top) to Martinique (bottom) from MODIS 215-threshold product (left), MOD09 product from WJ2016 (center), and the relief (right; 0–1200 m scale, red higher). Images have been adjusted for clearer reproduction and to emphasize the value of the additional resolution of the threshold product. Artifacts are present in the WJ2016 product – especially evident along coasts of Dominica (center island) and Martinique. A high-resolution version of this figure is available in the online Supporting Material.
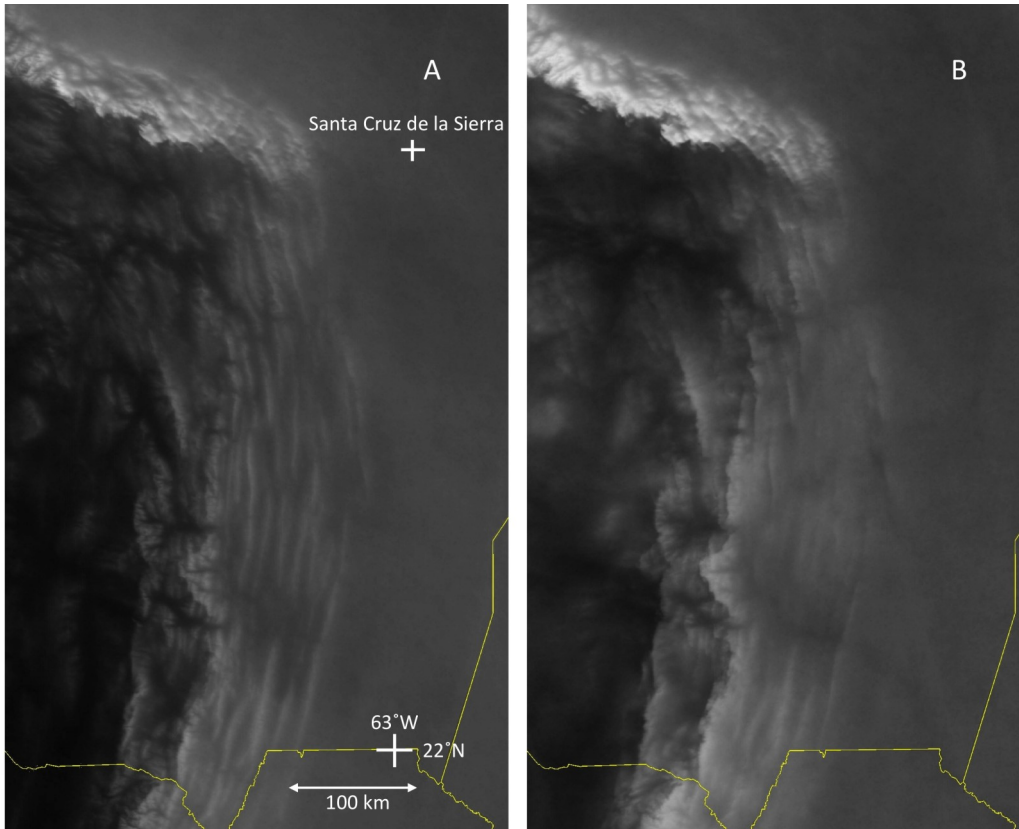
Figure 8. Comparison of mean annual cloudiness from A) Terra imagery (10:30 local time) and B) Aqua imagery (13:30 local time) for the Andean foothills of southern Bolivia. The mean Terra cloudiness reflects more closely the underlying terrain features because of the shallower atmospheric boundary layer at this time.

9 Our normalized cloud frequency difference is Aqua minus Terra annual mean cloudiness divided by annual mean cloudiness, then multiplied by 100 to obtain percent.
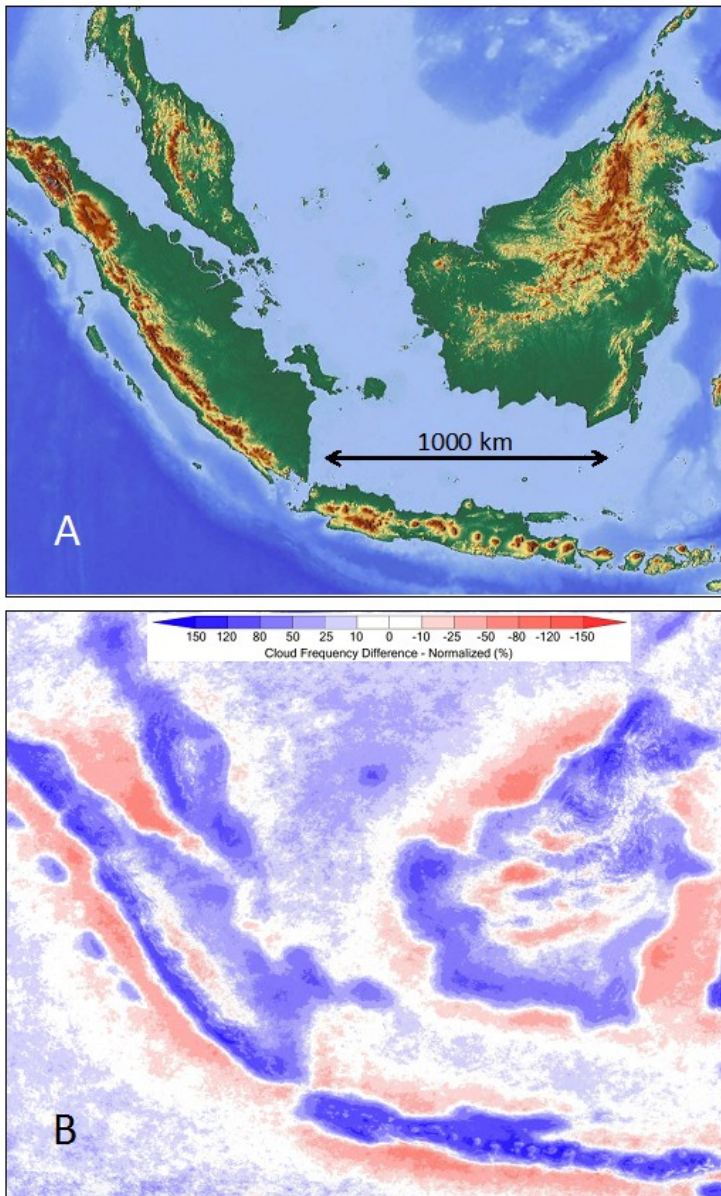
Figure 9. A) The relief for much of Malaysia and Indonesia and B) the annual mean Aqua (13:30 local time) minus Terra (10:30 local time) normalized cloud frequency difference[9]. Red shading indicates where cloudiness decreases between Terra and Aqua imagery times, blue is where it increases. The importance of the sea-breeze circulation is evident in suppressing daytime cloudiness offshore and increasing it over inland coastal areas. Mountain–valley circulations are also important in modulating daytime cloudiness away from coastal areas.

atmospheric boundary layer (Figure 8). As solar radiation heats the surface, convective currents progressively deepen the atmospheric boundary (well-mixed) layer. If sufficient moisture is available, clouds will form in the coolest air near the top of this boundary layer. Initially, the cumulus clouds forming will be shallow – close to the surface. As such they tend to reflect the underlying terrain variations, with clouds forming first over hills or slopes (Figure 8A). As daytime solar heating proceeds the atmospheric mixed layer continues to deepen and cloud bases tend to be higher and the clouds extend over a deeper layer. The clouds may also be displaced with the prevailing winds. Thus

the Aqua-based mean cloudiness estimates (Figure 8B) reflect the topographic relief somewhat less than do estimates from Terra imagery.

Diurnal mid-day tendencies

The differences between the Terra and Aqua mean cloudiness can provide insight into the physical processes responsible for the MODIS mean cloudiness patterns. Figure 9 shows the difference between the Aqua and Terra cloudiness for the boreal summer over the region of the western 'Maritime Continent' – including Borneo, Sumatra, Java and the Malay Peninsula. This prod-

9 Our normalized cloud frequency difference is Aqua minus Terra annual mean cloudiness divided by annual mean cloudiness, then multiplied by 100 to obtain percent.
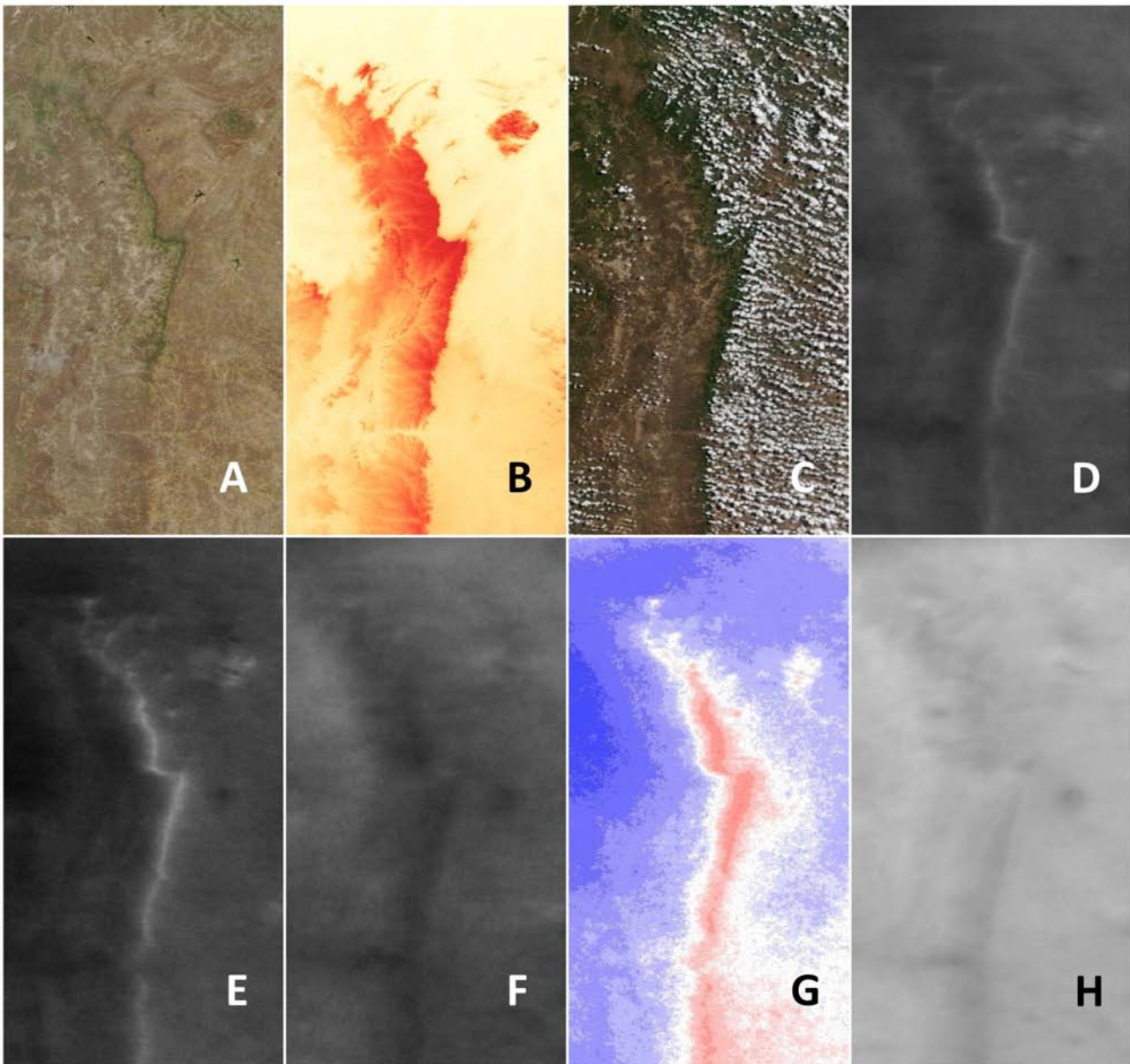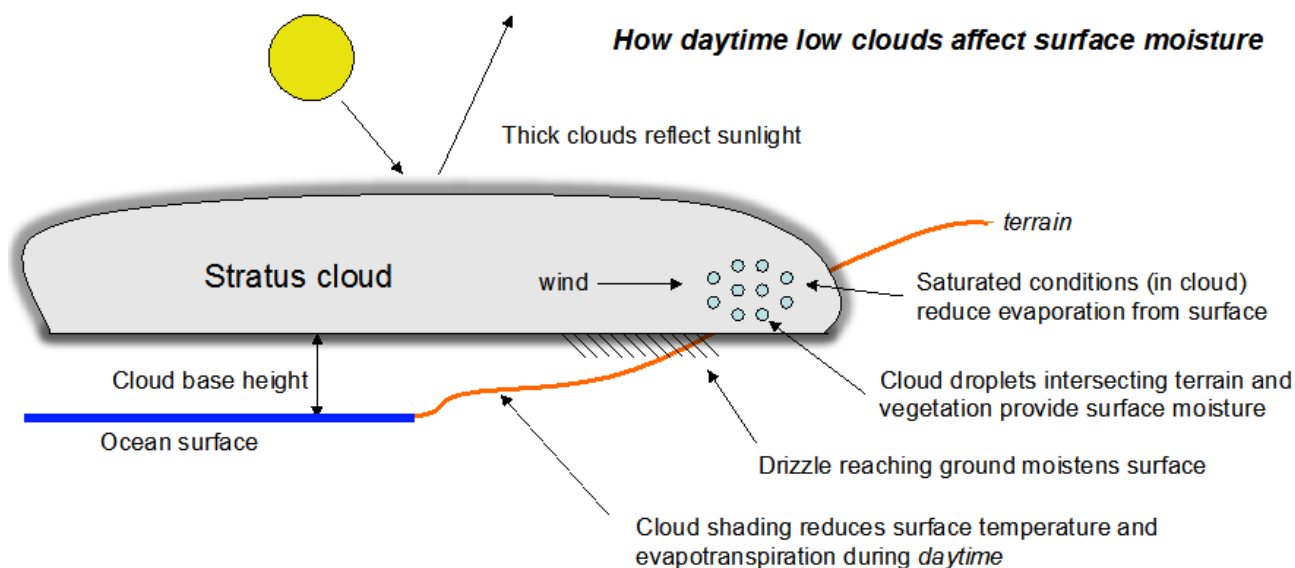
Figure 10. Escarpment in northeast Brazil (view centered ~ 4.5˚ S 41.5˚ W); scene is ~280 km North–South. A) MODIS Terra true color view on Nov 10 2014 showing green escarpment vegetation; B) elevation (0–1200 m color scale, darker red is higher; C) MODIS Terra true color image on July 13 2016 showing clouds (moving from east) ending at escarpment; D) mean annual cloudiness for Aqua + Terra using 215 threshold; E) same as D except only for Terra (note the prominent cloud enhancement at the escarpment location); F) same as E but for Aqua (the escarpment cloud signature has essentially disappeared); G) the Aqua–Terra difference – red indicates decreasing cloudiness from Terra to Aqua times, blue the opposite; H) MOD09 average cloudiness from WJ2016 for same area – the escarpment cloudiness signature is weak.

uct, reflecting the 3-h change in cloudiness between 10:30 LT and 13:30 LT, shows that cloudiness has generally decreased over the coastal regions of much of Borneo and Java while inland areas and mountain slopes have increased in cloudiness. These changes reflect sea- and slope-breezes and their associated vertical circulations that tend to either enhance or suppress cloud development (Defant 1951, Estoque 1962, Pielke

1974, Atkinson 1981, Zhou and Wang 2006). The sea-breeze signature, depicted best by the Aqua minus Terra product, is evident along most tropical coastlines, especially in regions of more frequent cloudiness.

Having separate climatologies from the Terra and Aqua satellites can be useful. Figure 10 shows the mean annual cloudiness for a part of northeastern Brazil encompassing a north–south

How daytime low clouds affect surface moisture

Thick clouds reflect sunlight

Stratus cloud

wind

terrain

Saturated conditions (in cloud) reduce evaporation from surface

Cloud base height

Ocean surface

Cloud droplets intersecting terrain and vegetation provide surface moisture

Drizzle reaching ground moistens surface

Cloud shading reduces surface temperature and evapotranspiration during *daytime*

Figure 11. Schematic showing how stratus clouds can impact the underlying surface.

escarpment that supports semi-evergreen forest not found in the surroundings (Figure 10A). Although the topographic relief (Figure 10B) is modest, with terrain rising from about 200 m east of the escarpment to 800 m ASL to the west, it is still sufficient to strongly modulate cloudiness (Figure 10C–D). The mean Terra cloudiness (E) defines the upslope of the escarpment clearly while only three hours later the Aqua mean cloudiness lacks this maximum. The difference between the Aqua and Terra cloudiness (Figure 10G) shows that the cloudiness decreases during the mid-day along the escarpment, but increases on either side. Curiously, the escarpment cloudiness signature is barely evident in the WJ2016 product (Figure 10H), unlike the mean from the 215-threshold product (Figure 10D).

The closer relationship between Terra mean cloudiness and terrain is potentially important for predicting fog-drip on coastal terrain, or on interior mountain ranges in specific regions of upslope motion such as northeast Brazil or parts of West (or East) Africa. Since sunlight has had less time to heat and deepen the atmospheric boundary layer, the Terra cloudiness is likely to better represent late night or early morning cloudiness patterns than the Aqua mean cloudiness fields. One might expect that fog-drip environments would also be

more closely related to Terra mean cloudiness fields, since cloud bases over land would be lower at this time. In summary, there is potentially valuable information in the separate Terra and Aqua cloudiness fields.

Biogeographical applications of MODIS-based cloud climatologies

Cloudiness around subtropical islands and coastlines

WJ2016 compared known tropical cloud forest locations with MODIS cloud frequency distributions, showing a relatively close relationship. Here we restrict our discussion to showing the value of MODIS climatologies in describing cloud-impacted environments on subtropical and tropical islands immersed in stratus for parts of the year when little conventional precipitation falls.

Stratus clouds are layered clouds generally found at the upper part of the atmospheric boundary layer and capped by a temperature inversion that inhibits much vertical displacement of air. The tops of such cloud layers are usually found between 500 m and 2 km ASL (Albrecht et al. 1995, Zuidema et al. 2009) and are thus more strongly affected by the underlying topography than are clouds that are either found at high altitudes (e.g. cirrus) or those that have large vertical extent (e.g. cumulonimbus).

Stratus clouds are comprised of cloud drop-
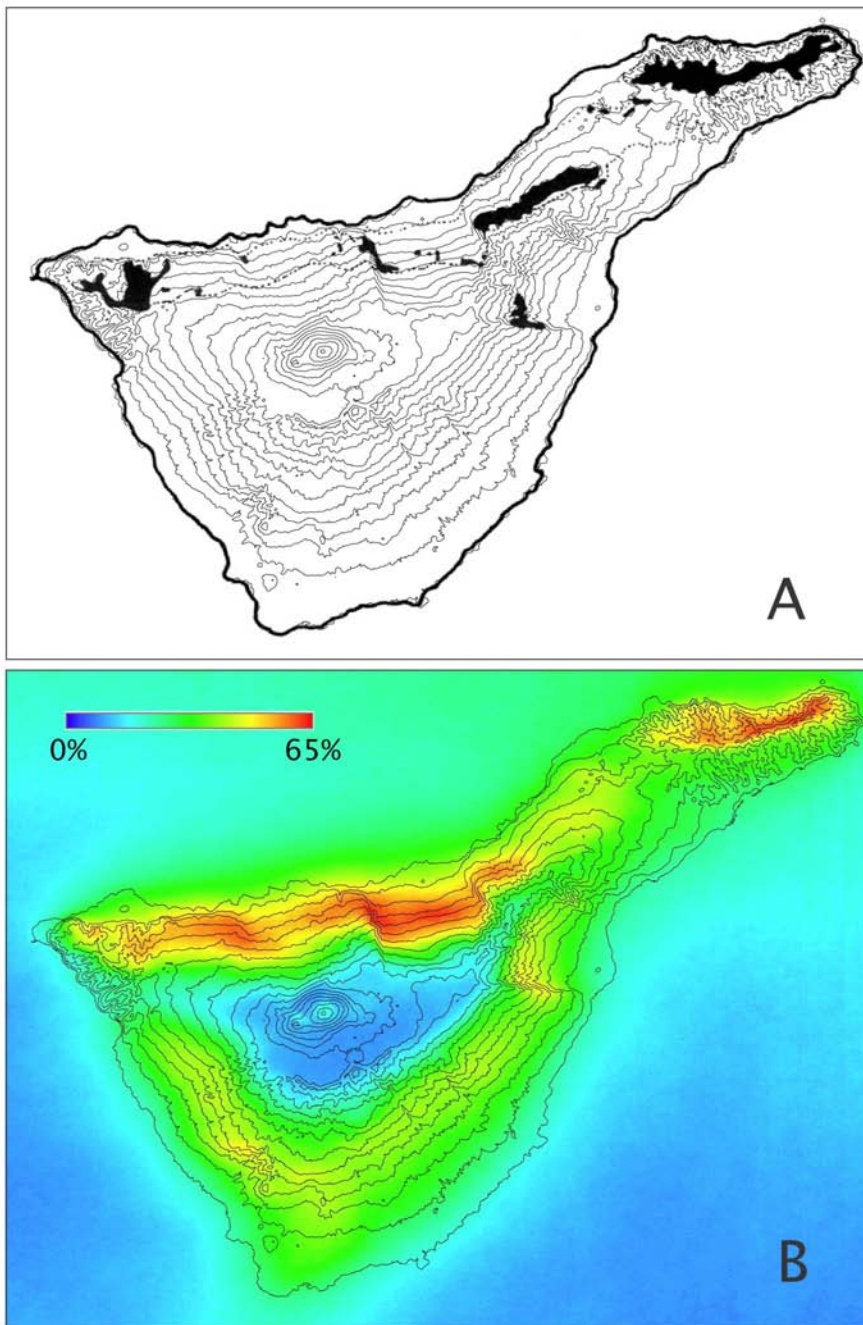
Figure 12. Island of Tenerife in the Canary Islands with elevation contours every 200m; image is ~83km across. A) The current (black areas) and historical (enclosed by thin dashed lines) distribution of laurisilva (moist) forests (after Santos 1990 and Arévalo et al. 2011). B) The annual mean cloudiness from the 215-threshold product. Close agreement between areas of high cloud frequency and laurisilva forests is apparent.

lets that are small enough (~10 microns) to have near-negligible terminal velocity. Figure 11 shows schematically some of the main impacts of stratus on an underlying surface. Horizontal wind in the cloud layer with a component towards the terrain will result in some droplets impacting and wetting the surface – often called 'horizontal rain' or 'fog drip'. The stronger the horizontal wind towards the terrain the greater the surface wetting. If the stratus is thick enough, drizzle (light rain) will form within the stratus, fall out, and further moisten the surface. Even with near-calm conditions, the presence of cloud on the surface ('fog'), with near-

saturated conditions (100% relative humidity), ensures that there is little evaporation from the surface or through leaf stomata. While many aspects of the interaction of stratus with the underlying surface are complex (including the turbulent interaction of wind with topography, the surface wetting by cloud droplets, and the formation of drizzle from stratus) the importance of cloud-related impacts are readily apparent along many arid coasts and around subtropical islands.

Well-known archipelagos frequently immersed in stratus (or shallow trade wind cumulus) include the Azores, Canaries, and Cape Verde is-

lands in the northeastern Atlantic, and the Galapagos and Hawaiian Islands in the Pacific. Figure 12 shows an example of the strong control that the topography of Tenerife, the largest island in the Canaries, has on the distribution of the cloudiness. The association of this frequent cloudiness with the distribution of unique laurisilva forests and other mesic vegetation in the Canary islands has been much discussed (e.g. Fernández-Palacios 1992, Fernández-Palacios et al. 1995, 2011). The current and historical moist forest distribution on Tenerife (Figure 12a) is closely associated with the MODIS areas of greatest cloud cover (Figure 12b). Similar close agreements are found on the other western Canary Islands where the islands extend into the cloud layer.

Stratus and fog drip also strongly impact the coastlines of California (Azevedo and Morgan 1974, Fischer et al. 2009, Hiatt et al. 2012), Baja California (Garcillan et al. 2012), and the coast-

lines of Peru and Chile (Pinto et al. 2006, Cereceda et al. 2008, Borthagaray et al. 2010, Hesse 2012, Muenchow et al. 2013). Favorably exposed portions of the coastline of Peru and northern Chile are often vegetated islands in an otherwise hyperarid Atacama coastal desert (Figure 13). A quantification of these coastal 'cloud oases', evaluating seasonality, inter- and intra-annual variability and diurnal variations, akin to that done for 'hotspots of cloud stability' by WJ2016, should be straightforward.

The value of the MODIS-based cloud climatologies for explaining vegetation distribution relative to some other products available to the biogeographic/conservation communities is illustrated in Figure 14. Isabela is the largest of the Galapagos Islands and is immersed in moist winds from the southeast for much of the year. The interaction of low-level air flow with the island's topography (Figure 14A) produces regions of enhanced
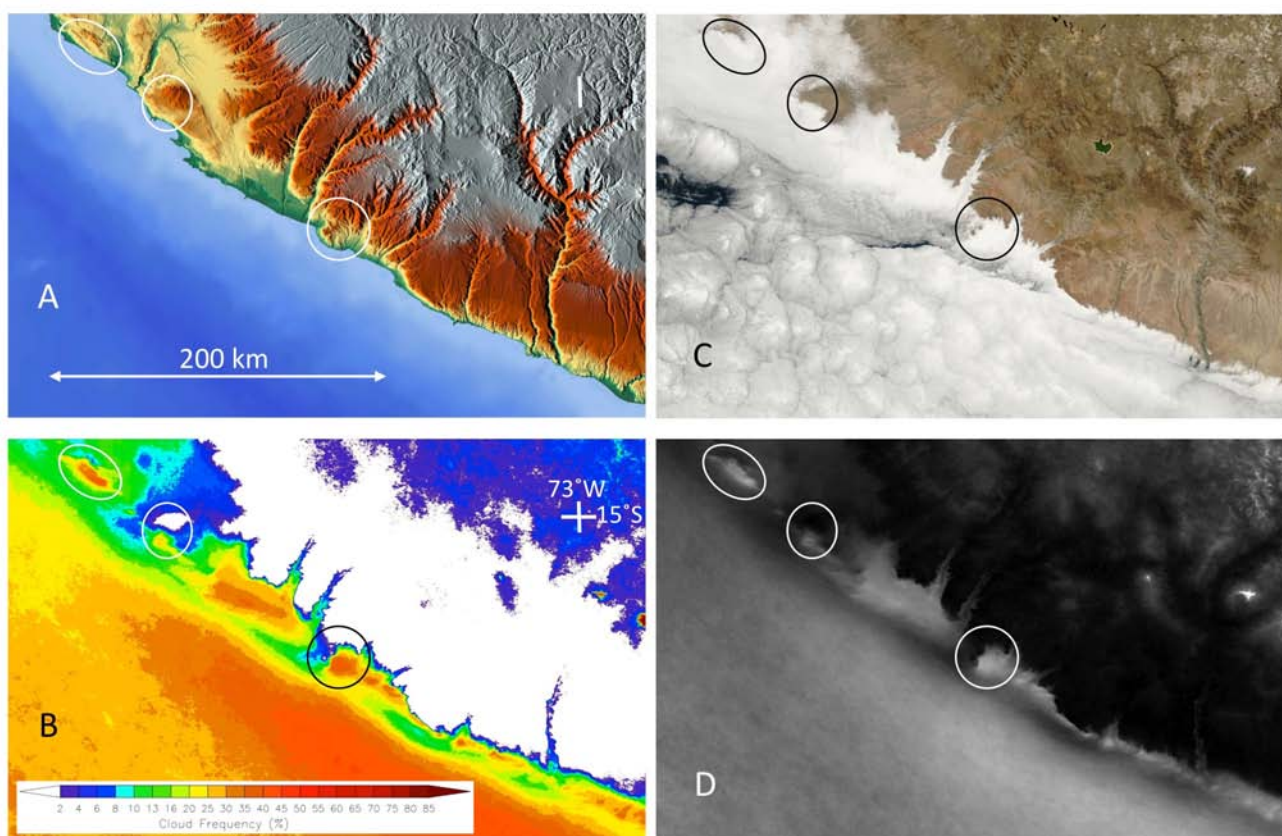
Figure 13. The importance of coastal relief in modulating cloudiness along stratus-dominated coasts. A) topography along the south Peruvian coastline; B) 215-threshold mean annual Aqua+Terra cloudiness with color scale; C) cloudiness in one individual Terra image; and D) grayscale mean annual Aqua+Terra cloudiness that better shows subtle differences in cloudiness. The circles in each image show areas of prominent coastal relief associated with maxima in mean annual cloudiness. Note similarity of individual day cloudiness (C) to mean cloudiness in B and D. The circle near the center depicts the Lomas de Atiquipa, one of the most biodiverse regions along the Peruvian coastline.

and suppressed cloudiness (Figure 14B). The humid forest distribution (Figure 14C, modified from Trueman and Ozouville 2010) closely matches this annual mean cloudiness pattern. This is in contrast to multi-year rainfall climatologies from the Tropical Rainfall Measuring Mission (TRMM) satellite (Figure 14D, data from Bookhagen[10]) that are unrealistic in areas that are dominated by light rain such as the Galapagos. It also contrasts with clima-

tologies from the widely-used WorldClim (Hijmans et al. 2005) (Figure 14E), which, because of insufficient observational data, unrealistically mirror the topography (Figure 14F). Though not shown in Figure 14, the annual cloudiness from WJ2016 shows good agreement with the threshold-based results. Relatively fewer high albedo surface artifacts are expected in the Galapagos Islands because of their dark volcanic landscapes.
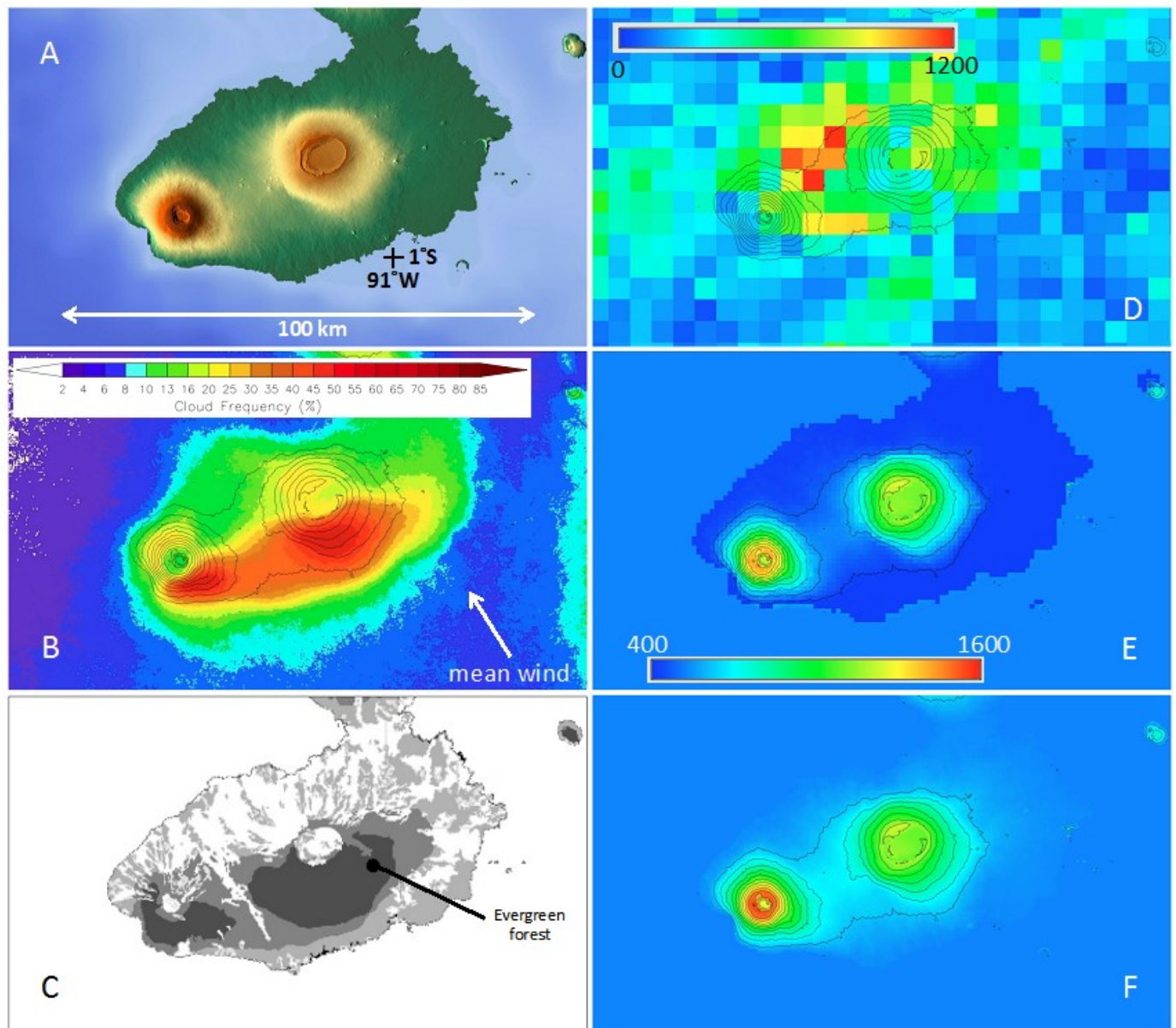
Figure 14. The southern part of the island of Isabela in the Galapagos, showing different products that can be related to the observed vegetation cover. A) shaded relief showing two prominent volcanoes together with scale and latitude/longitude; B) MODIS-based annual mean cloudiness from Aqua and Terra imagery using a 215 cloud-detection threshold (mean near-surface wind direction is shown schematically by the arrow); C) schematic vegetation cover after Figure 3 in Trueman and d'Ozouville (2010); D) TRMM-based annual mean precipitation (scale in mm) with pixels of 4 km (TRMM radar native resolution[10]); E) WorldClim-based annual mean precipitation in mm; and F) elevation. Contour interval in B and D–F is 150 m. The domain is identical in all figures and is ~119 km across.

10 Data from http://www.geog.ucsb.edu/~bodo/TRMM/, last accessed September 14, 2016

Conservation applications

Although cloud forests can be imaged directly using high-resolution (~1 m) commercial satellites, the monthly mean MODIS cloudiness data allow for quantification of the variability of cloudiness, including aspects of its temporal variability. Such a diagnostic analysis was carried out by WJ2016 for the nearly complete record of MODIS. A diagnosis of the diurnal variability of cloudiness (difference between the Terra (~10:30 LT) and Aqua (~13:30 LT) averages would also be useful, since some regions are more cloudy in the morning than in the afternoon, and vice-versa. In fact, cloudiness patterns in the morning (Terra-based) might represent early morning and late-night cloudiness patterns better than the mean cloudiness fields, and thus reflect better the distribution of forests dependent on fog drip than would the mean cloudiness fields. However, this needs to be shown. Thus, as noted by WJ2016, areas with minimal diurnal, seasonal and interannual cloud frequency variability might be expected to favor species requiring continuous moisture, whereas cloud forests with larger seasonal or diurnal variations in cloudiness might favor different species compositions.

One use of MODIS cloudiness data for conservation applications may be to help reconstruct cloud forest distributions in fully deforested areas, such as parts of the Mata Atlantica in Brazil, or moist forests of eastern Madagascar. Current MODIS-based cloud climatologies can be used to infer the pre-deforestation cloud forest distribution *if* the current annual cloudiness is closely related to cloud forest distributions. This presumes that the mean cloudiness is mainly forced by atmosphere–topography interactions and minimally affected by variations in land-cover characteristics (i.e. deforestation doesn't importantly affect the mean cloudiness).

An immediate *qualitative* application of available MODIS climatologies is to aid field sampling. As described in WJ2016, areas of minimum annual and interannual cloudiness reflect stability of the cloudiness field – which might (or might not) argue for greater biodiversity. There are still many remote tropical mountainous areas where

the efficiency of rapid assessment programs (Alonso et al. 2011) might be improved, or new explorations motivated, by reference to such climatologies.

Summary and recommendations

We have discussed aspects of recent high spatial resolution cloud climatologies based on MODIS imagery, focusing on two procedures recently used for developing such climatologies. WJ2016 generated monthly mean cloud frequencies (and other quantities derivable from them) from a 1km cloud mask product previously developed by the MODIS research community to identify cloud-contaminated pixels. The other procedure uses a brightness threshold technique to identify bright pixels which are related to highly reflective (thick) clouds. Both procedures yield results that are similar in many aspects, yet have important differences. Neither product can be used as a surrogate for observed precipitation.

More work is needed to evaluate the best thresholds (or combination of thresholds) to detect cloudiness or to derive biogeographically useful products. There is unlikely to be a magical threshold or combination that works well for every region. Perhaps most feasible will be developing relationships between MODIS (and other satellite-based) climatologies with conventional climatological data such as those used to produce WorldClim. Given that clouds affect the underlying surface in multiple ways, attention is needed to develop relationships between cloudiness and biophysical quantities of importance to biogeographers, ecologists, and those with similar needs.

Regional calibration of MODIS-based climatologies, linking cloud frequency to physical quantities like mean precipitation, fog drip, diurnal temperature range, or surface solar radiation input should be possible with high spatial resolution validation networks. An example of the need for such field validation is shown in Figure 15. Despite the relatively close agreement between the two MODIS techniques, a precipitation climatology (Giambelluca et al. 2013) based on a relatively dense observation network shows that much lower precipitation (~1000 mm/yr) is associated
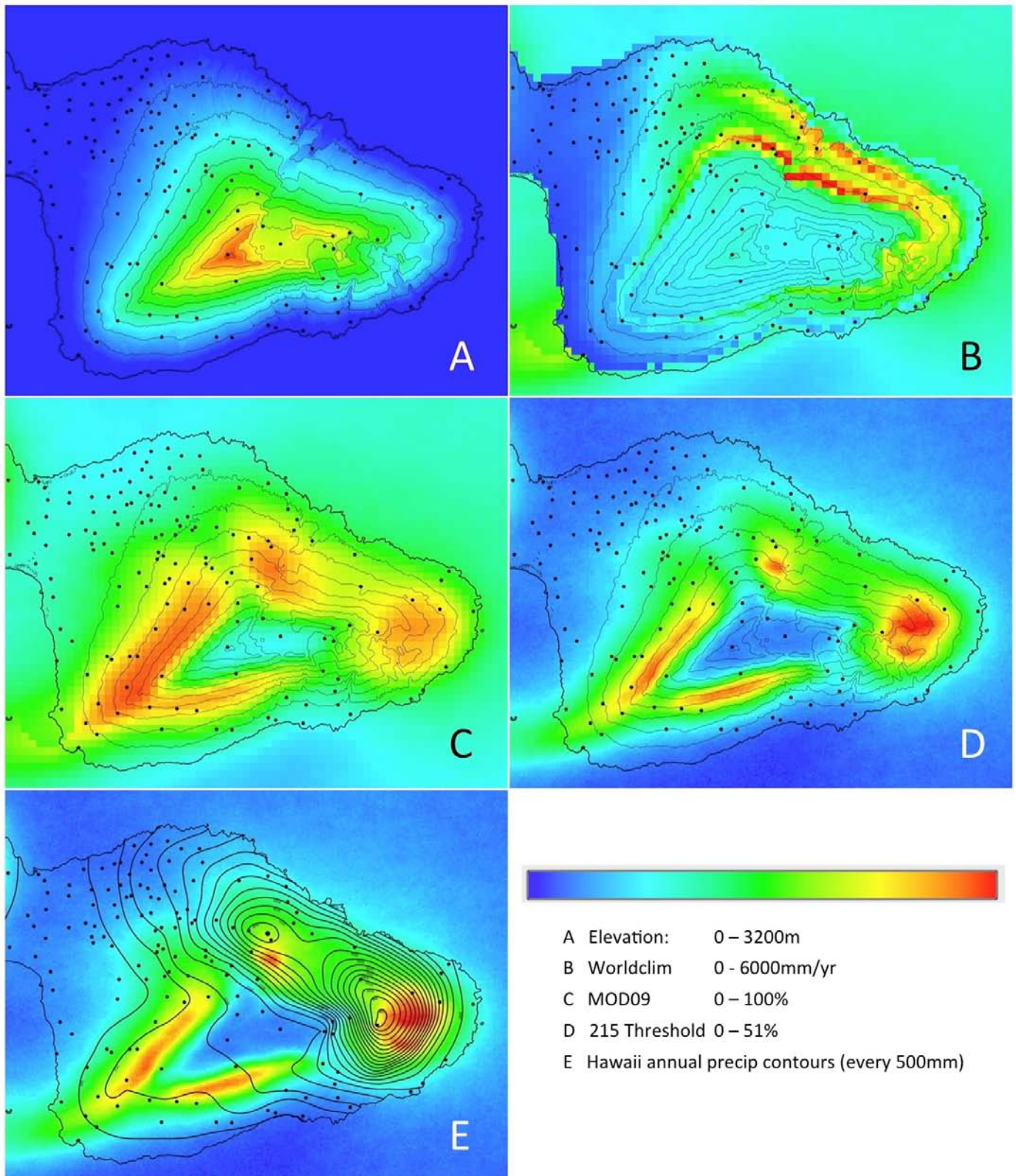
Figure 15. Eastern part of the island of Maui (~20.7° N, 156.2° W), showing: A) elevation (contours are 200 m interval on all panels), B) WorldClim mean annual precipitation (scale 0–6000 mm); C) MOD09 annual mean cloudiness from WJ2016 (0–100 %); D) 215 threshold-based climatology (scale is 0–51% to approximately match MOD09 pattern in C); and E) isohyets of mean annual precipitation from Giambelluca et al. (2013). Black dots are stations used in this analysis; WorldClim stations were much fewer. Contour interval is 500 mm, except for one contour at 750 mm/yr. Main features are 1) unrealistic WorldClim analysis, 2) good agreement between MODIS-based cloudiness products (note value of higher resolution with threshold product), 3) poor sampling with raingauges of cloudiness maxima, and 4) much lower rainfall suggested in leeside cloud maxima.

with the two lee-side bands of frequent cloudiness (on the northwest and south sides of the high terrain) compared with the windward maxima (~6000–9000 mm/yr). These lee-side regions of maximum cloudiness are evident on other high islands embedded in steady flow, including Hawaii (Figure 2) and Tenerife (Figure 12), where they also represent areas of lesser precipitation relative to their windward maximum. Clearly, even on the same island it is not possible to apply the same relationship between cloud frequency and precipitation. Some physical effects should be similar, such as reduction in solar radiation reaching the surface for similar frequencies of thick cloudiness. But the main processes responsible for the precipitation are clearly not the same.

Comparison of the station network used in developing the precipitation climatology shown in Figure 15E suggests that the centers or bands of maximum cloud frequency shown by the threshold-based procedure are not well sampled by the observations (Figure 15D). The windward precipitation *may* be offset to the east from the analyzed pattern and the amount may be even higher – *if* there is a relationship between cloudiness and precipitation in this region. Likewise, observations poorly sample the core of the lee-side bands of maximum cloudiness, so the analyzed precipitation along the elevation gradient *may* be unrealistic. The main point here is that the current MODIS climatologies show where key spatial gradients in cloudiness occur. We also know (considerably less precisely) the areas of maximum biodiversity (e.g. Barthlott et al. 2005). Thus, cloudiness–precipitation calibration transects can be selected to represent a variety of environments of greatest interest to the research or conservation communities. Actually carrying out such validation measurements can be complex, but need not require long-term monitoring, since, in regions where topography strongly modulates cloudiness, even short measurement periods can be representative of the actual climatology (e.g. Figure 2).

Acknowledgements

Author Contributions

Michael Douglas wrote the manuscript draft and supervised the overall activity. Rahama Beida processed much of the MODIS imagery and generated most of the figure materials. John Mejia revised the manuscript, developed the original software for cloud extraction from the MODIS imagery, and helped supervise summer students involved with MODIS-related work. Marcia Fuentes developed MODIS climatologies for Brazil and processed global wind field information for help in interpreting the mean cloudiness patterns.

References

Albrecht, B.A., Jensen, M.P. & Syrett, W.J. (1995) Marine boundary layer structure and fractional cloudiness. Journal of Geophysical Research, Atmospheres, 100, 14209–14222.

Alonso, L.E., Deichmann, J.L., McKenna, S.A., Naskreki, P. & Richard., S.J. (eds) (2011) Still counting…: biodiversity exploration for conservation: the first 20 years of the rapid assessment program. The University of Chicago Press, Chicago (distributed for Conservation International).

Arévalo J.R., Delgado J.D. & Fernández-Palacios J.M. (2011) Regeneration of potential laurel forest under a native canopy and an exotic canopy, Tenerife (Canary Islands). Forest Systems 20, 255–265.

Atkinson, B.W. (1981) Mesoscale atmospheric circulations. Academic Press, London.

Azevedo, J. & Morgan, D.L. (1974) Fog precipitation in coastal California. Ecology, 55, 1135–1141.

Barthlott, W., Mutke, J., Rafiqpoor, M.D., Kier, G. & Kreft, H. (2005) Global centers of vascular plant diversity. Nova Acta Leopoldina, 92, 61–83.

Borthagaray, A. I., Fuentes, M.A. & Marquet, P.A. (2010) Vegetation pattern formation in a fog-dependent ecosystem, Journal of Theoretical Biology, 265, 18–26.

Cereceda, P., Larrain, H., Osses, P., Farias, M. & Egaña, I. (2008) The Spatial and temporal variability of fog and its relation to fog oases in the Atacama Desert, Chile. Atmospheric Research, 87, 312–323.

Defant, F. (1951) Local winds. In: Compendium of meteorology (ed. By T.F. Malone), pp. 658–672. American Meteorological Society, Boston, USA..

Estoque, M.A. (1962) The sea breeze as a function of the prevailing synoptic situations. Journal of Atmospheric Sciences, 19, 244–250.

Fernández-Palacios, J.M. (1992) Climatic responses of plant species on Tenerife, the Canary Islands. Journal of Vegetation Science, 3, 595–602.

Fernández-Palacios, J.M. & de Nicolás, J.P. (1995) Altitudinal pattern of vegetation variation on Tenerife. Journal of Vegetation Science, Vol. 6, 183–190.

Fernández-Palacios, J.M., Nascimento, L., Otto, R., Delgado, J.D., Garcia-del-Rey, E., Arevalo, R. & Whittaker, R.J. (2011) A reconstruction of Palaeo-Macaronesia with particular reference to the long-term biogeography of the Atlantic island laurel forests. Journal of Biogeography, 38, 226–246.

Fischer, D.T., Still, C.J. & Williams, A.P. (2009) Significance of summer fog and overcast for drought stress and ecological functioning of coastal California endemic plant species. Journal of Biogeography, 36, 783–799.

Garcillan, P.P., Vega, E. & Martorell, C. (2012) The *Brahea edulis* palm forest in Guadalupe Island: a North American fog oasis? Revista Chilena de Historia Natural, 85, 137–145.

Giambelluca, T.W., Chen, Q., Frazier, A.G., Price, J.P., Chen, Y.-L., Chu, P.-S., Eischeid, J.K. & Delparte, D.M. (2013) Online rainfall atlas of Hawaii. Bulletin of the American Meteorological Society, 94, 313–316.

Hesse, R. (2012) Spatial distribution of and topographic controls on *Tillandsia* fog vegetation in coastal southern Peru: remote sensing and modelling. Journal of Arid Environments, 78, 33–40.

Hiatt, C., Fernandez, D. & Potter, C. (2012) Measurements of fog water deposition on the California Central Coast. Atmospheric and Climate Sciences, 2, 525–531.

Hijmans, R.J., Cameron, S.E., Parra, J.L., Jones P.G. & Jarvis, A. (2005) Very high resolution interpolated climate surfaces for global land areas. International Journal of Climatology, 25, 1965–1978.

Kanan C. & Cottrell G.W. (2012) Color-to-grayscale: does the method matter in image recognition? PLoS ONE, 7(1), e29740.

Karlsson, K.-G. (2002) A 10 year cloud climatology over Scandinavia derived from NOAA advanced very high resolution radiometer imagery. International Journal of Climatology, 23, 1023–1044.

Muenchow, J., Brauning, A., Rodriguez, E.F. & von Wehrden, H. (2013) Predictive mapping of species richness and plant species distributions of a Peruvian fog oasis along an altitudinal gradient. Biotropica, 45, 557–566.

Pielke, R.A. (1974) A three-dimensional numerical model of the sea breezes over south Florida. Monthly Weather Review, 102, 115–139.

Pinto, R., Barria, I. & Marquet, P.A. (2006) Geographical distribution of *Tillandsia lomas* in the Atacama Desert, northern Chile. Journal of Arid Environments, 65, 543–552.

Platnick, S., King, M., Ackerman, S., Menzel, W., Baum, B., Riedi, J. & Frey, R. (2003) The MODIS cloud products: algorithms and examples from Terra. IEEE Transactions on Geoscience and Remote Sensing, 41, 459–473.

Santos A. (1990) Bosques de laurisilva en la región macaronésica. Consejo de Europa. Serie Naturaleza Y Medio Ambiente, 49, 1–79.

Stubenrauch, S.C., Guignard, A. & Lamquin, N. (2010) A 6-year global cloud climatology from the Atmospheric Infrared Sounder AIRS and a statistical analysis in synergy with CALIPSO and CloudSat. Atmospheric Chemistry and Physics, 10, 7197–7214.

Stubenrauch C.J, Rossow, W.B., Kinne, S. et al. (2013) Assessment of global cloud datasets from satellites: project and database initiated by the GEWEX Radiation Panel. Bulletin of the American Meteorological Society, 94, 1031–1049.

Trueman, M. & d'Ozouville, N. (2010) Characterizing the Galapagos terrestrial climate in the face of global climate change. Galapagos Research, 67, 26–37.

Vermote, E.F., S.Y. Kotchenova & J.P. Ray (2011) MODIS surface reflectance user's guide. http://modis-sr.ltdri.org

Wilson, A.M., Parmentier, B. & Jetz, W. (2014) Systematic land cover bias in Collection 5 MODIS cloud mask and derived products – a global overview. Remote Sensing of Environment, 141, 149–154.

Wilson, A.M. & Jetz W. (2016) Remotely sensed high-resolution global cloud dynamics for predicting ecosystem and biodiversity distributions. PLoS Biology 14: e1002415.

Zuidema, P., Painemal, D., de Szoeke, S., & Fairall, C. (2009) Stratocumulus cloud-top height estimates and their climatic implications. Journal of Climate, 22, 4652–4666.